Colour Metallography of Cast Iron

By Zhou Jiyang, Professor, Dalian University of Technology, China
Translated by Ph.D Liu Jincheng, Fellow of Institute of Cast Metal Engineers, UK

Note: This book consists of five sections: Chapter 1 Introduction, Chapter 2 Grey Iron, Chapter 3 Spheroidal Graphite Cast Iron, Chapter 4 Vermicular Cast Iron, and Chapter 5 White Cast Iron. CHINA FOUNDRY publishes this book in several parts serially, starting from the first issue of 2009.

Chapter 3

Spheroidal Graphite Cast Iron (IV)

3.7 Segregation of SG iron

The non-uniform distribution of solute elements during solidification results in the micro segregation of SG iron. As for the redistribution of elements in the phases of the solidification structure, there is no intrinsic difference between SG iron and grey iron [132]. However, the author considered that the segregation of SG iron has received more focus, due to following reasons:

(a) The non-uniform distribution phenomena of solute elements in SG iron is more severe than in grey iron.

(b) The detrimental effect of non-uniform structure due to segregation on mechanical properties is more sensitive in SG iron, than in grey iron.

(c) Alloying elements are widely used in SG iron.

3.7.1 Segregation behaviour of elements in SG iron

(1) Segregation coefficient K_s

The segregation coefficient K_s of an element in the dendrites of SG iron is defined as:

K_s = *element concentration in the centre of dendrites / element concentration in the intercellular dendrites*

However the K_s for eutectic grains in SG iron is slightly different from that in grey iron. Since there are a variety of definitions for eutectic grains in SG iron, a definition for K_s of a eutectic grain becomes very difficult. In order to give a quantitive description on segregation of SG iron, a definition on the simplest solidification unit is used; i.e. one graphite spheroid + austenite shell = one eutectic grain. Thus,

K_s= *element concentration in the austenite adjacent to the surface of a graphite spheroid* / element concentration in the outer rim of the austenite shell

Table 3-19 lists the values of segregation coefficient K_s for some elements. Due to different experimental conditions, the values in the table show quite a big difference from each other. Comparing the values in Table 3-19 with that in Table 2-6, it can be seen that the segregation degree of elements in SG iron is more severe than that in grey iron.

The distribution rule in SG iron is similar to that in grey iron. The negative segregation elements (K_s<1), Si, Cu, Ni, Co and Al are preferentially distributed in the austenite crystal surrounding graphite spheroids; the positive segregation elements (K_s>1), Mn,

Table 3-19: Segregation coefficient K_s of some elements in SG iron

Solute element	Literature				
	[133]	[134]	[135]	[※]	[※※]
Cu	10	5.10	4.86	7.50	
Ni	3.33	1.82	3.00		
Si	1.43	2.27	1.39	2.40	1.40
Ti	0.04			0.014	
Mo	0.039	0.0053⊙	0.058		
Cr	0.086	0.108	0.28	0.10	0.27
V	0.075			0.10	0.083
Mg		0.387		0.16	0.187
Mn	0.29 — 0.59		0.283	0.155	0.143

Note: casting condition: [133] not given; [134] sand mould, Φ 30 mm bar, ⊙-compound; [135] Φ12 mm, cooled in quartz tube; [※] the author's work, sand mould, Φ 160 mm; [※※] the author's work, thickness 25 mm, sand mould

Mo, Cr, P, V and Ti are enriched in the remaining intercellular liquid. The segregation behaviour of C is influenced by Si, because the negative segregation elements preferentially enter the austenite, which reduce the solubility of carbon in austenite; thus C is pushed to *LTF* areas and shows a positive segregation behavior.

(2) Variation in element segregation with solidification progress

During the progress of solidification, the content of various solute elements in solid, liquid and at S/L interface varies differently. Figure 3-86 shows the liquid quenched microstructures at different stages. *A* is the earliest precipitated solid, *B* is at the S/L interface and *C* is the un-solidified liquid. Figure 3-87 shows the variation rule of element content in the positions *A*, *B* and *C* with the progress of solidification. It can be clearly seen that:

(a) The content of solute elements around graphite spheroids (position *A*) does not change with the variation of solid phase fraction, showing that the diffusion of elements in solid is very small. The actual content (*C*) of negative-segregation elements Ni, Cu and Si at position *A* is higher than that of the liquid average (C_0), leading to $C/C_0 > 1$; among these, the relative concentration of Ni and Cu is higher than that of Si. The content (*C*) of positive-segregation elements Mo, Cr and Mn in austenite is lower than that of the liquid average (C_0), resulting in $C/C_0 < 1$; of these, Mo is the lowest, next is Cr followed by Mn.

(b) With increasing solid fraction, the content of Ni, Cu and Si around the solid edge (position *B*) decreases, whilst the concentration of Mo, Cr and Mn gradually increases.

(c) In the liquid phase (point *C*), at the beginning of solidification (solid fraction is 0%), the content of each element (*C*) is the same as the initial content of each element (C_0), $C/C_0 = 1$. With the progress of solidification, the volume of liquid is diminished and the positive elements in the liquid are gradually enriched, with segregation order: Mo > Cr > Mn. However, the negative-segregation elements Ni, Cu and Si are gradually depleted with the segregation sequence of Cu > Ni > Si.

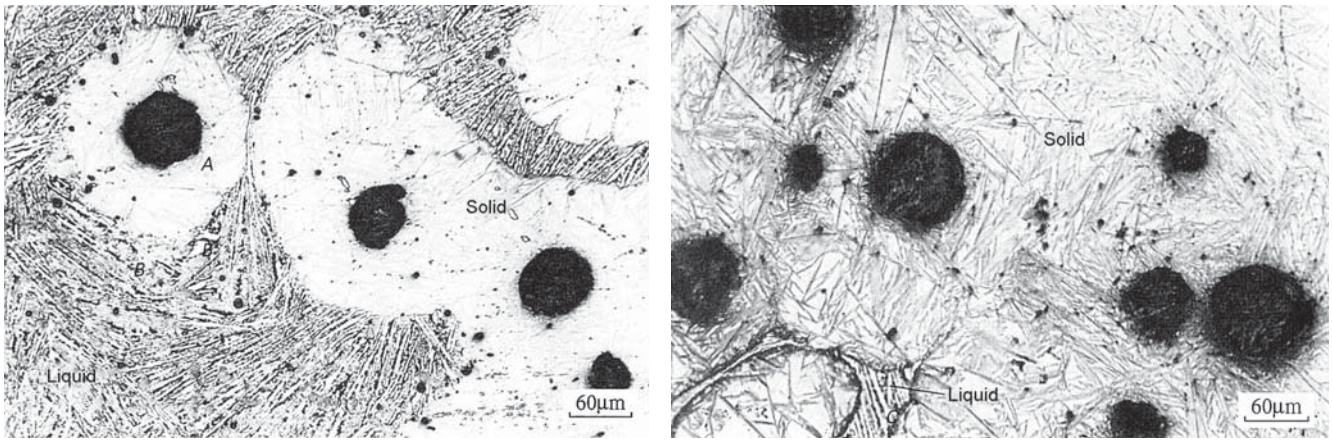

(a) Initial stage: *A* – the earliest precipitated solid around spheroids, *B* – at the S/L interface

(b) Final solidification stage: *C* – un-solidified liquid

Fig. 3-86: Liquid quenched microstructure at the different solidification stages

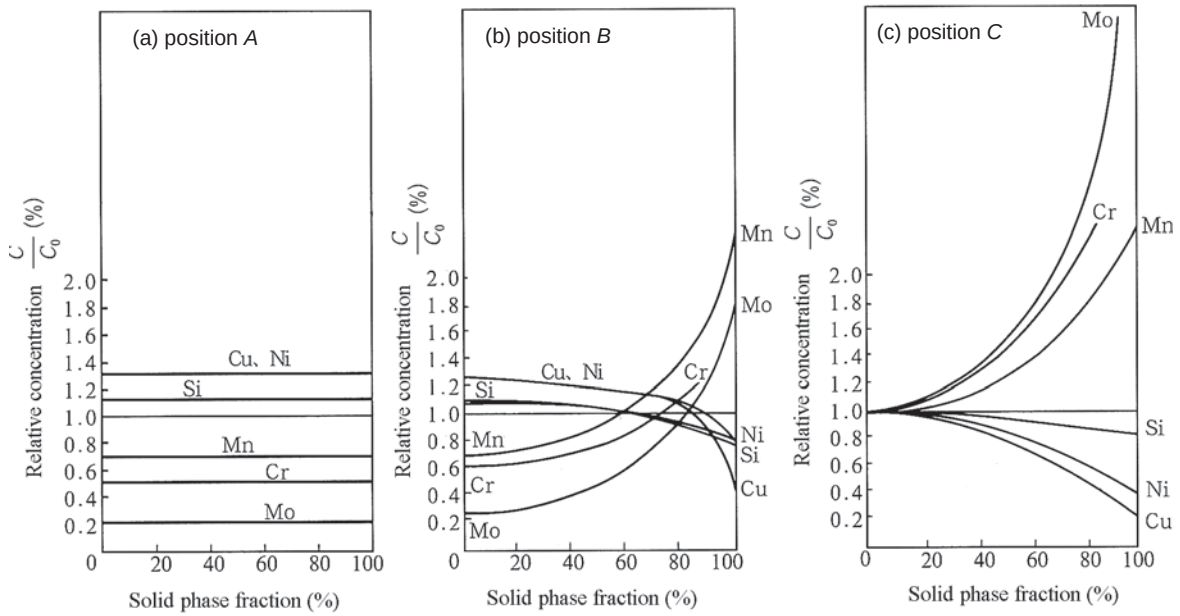

Fig. 3-87: Variation of solute element content at positions *A*, *B* and *C* shown in Fig. 3-86, with the progress of solidification
(Iron melt composition (mass%): C = 3.65%, Si = 2.45%, Mn = 0.41%, Cu = 0.91%, Mo = 0.83%, Cr = 0.50%, Ni = 0.83%. *C*- Actual content; C_0-Average content; Sample size: Φ12 mm.)

(3) Segregation of elements in the liquid channels

The austenite shell around a graphite spheroid consists of several austenite grains, between which are liquid channels. The author established that the concentration of positive-segregation elements is generally higher in the liquid channels, being the highest in the remaining liquid, see Fig. 3-88. In addition, it was found that the low melting point elements are readily enriched in the remaining liquid.

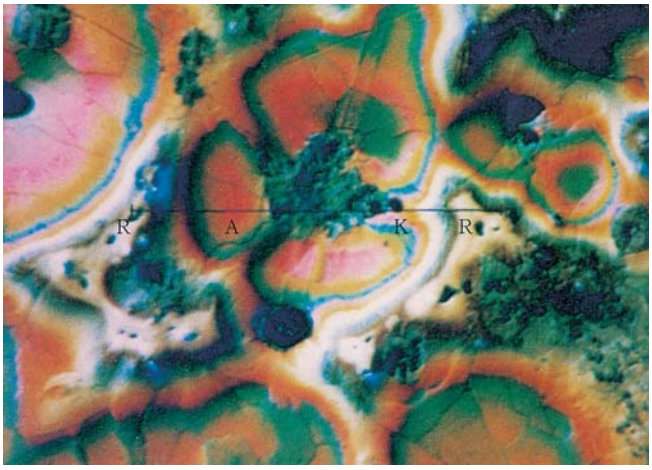

(a) Position of electron probe: G–graphite spheroid, A–austenite, K–liquid el, R–remaining liquid

(b) Distribution of elements

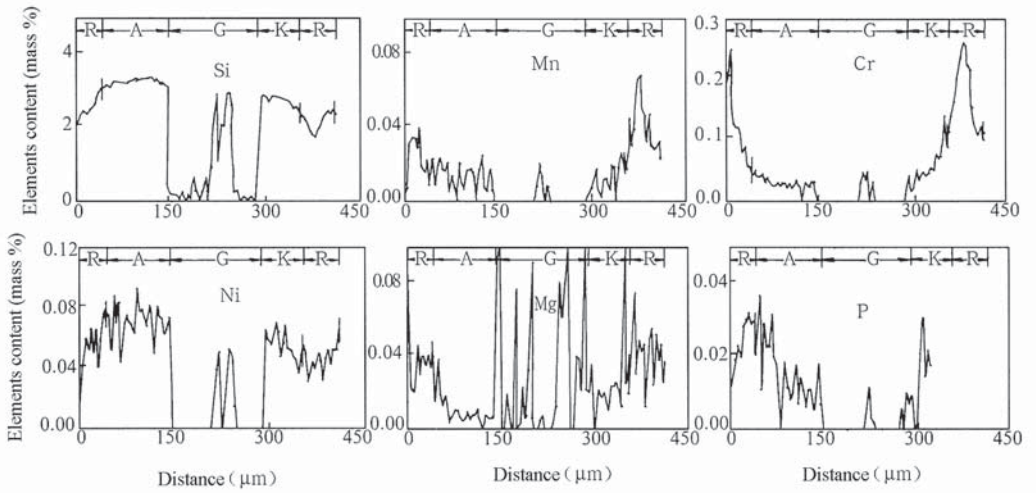

Fig. 3-88: Distribution of elements in the liquid channels

(4) Intercellular segregation

The slow cooling austenite dendrites in heavy section SG iron are well developed (the longest one can reach 70 mm), and arranged along the direction of heat flow. The positive elements in the remaining liquid between the dendrites are enriched continuously and form intercellular segregation. Figure 3-89 shows the measurement positions of slow cooling dendrites in a heavy section SG iron and Table 3-20 lists the results of electron probe microanalysis in the dendrites and intercellular regions. The measured data show that Cr, Mn, Ti and P are higher in the intercellular regions and negative element Si is concentrated within the dendrites.

3.7.2 Factors affecting element segregation in SG iron

(1) The type and concentration of solute elements

The segregation tendency of solute elements in SG iron differs from each other. The strong carbide-forming elements have a large positive-segregation tendency, with the order of V > Cr > Mn [136]. Graphitising elements in SG iron exhibit negative-segregation features, but do not follow the graphitising sequence: Si > Ni > Cu. The K_s of Cu and Ni is larger than that of Si, and their relative content is higher than that of Si in austenite. Probably, this is related to the size of their atom radius: the radius of Si is 0.134 nm; that of Cu is 0.128 nm and Ni 0.124 nm. It can be seen from the large quantity of measured data that the degree of segregation of positive-segregation elements Mo, Cr and Mn is stronger than that of negative-segregation elements Cu, Ni and Si (see Fig. 3-87 and Table 3-19). The effect of element content on segregation shows that with increasing mass percent content, the segregation becomes more pronounced. Take Mn for example, with an increase from 1.5% to 2.0% (by weight), the percentage of Mn in the intercellular regions increases from 3.2% to 4.5%, see Fig. 3-90[137]. When the section thickness increases the effect of concentration is even stronger.

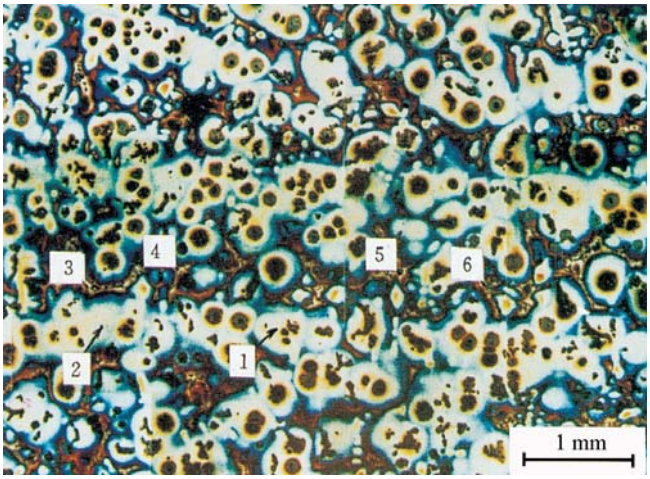

Fig. 3-89: Measurement position of intercellular segregation of slow-cooling dendrites:
1, 2–within dendrites; 3, 4, 5, 6–between dendrites

(2) Cooling rate

Increasing the cooling rate can significantly increase nodule

Table 3-20: Distribution of Si, Cr, Mn, Ti, P and S within and between dendrites (mass %)

Position		Si	Cr	Mn	Ti	P	S
Within dendrites	1	3.06	0.0236	0.25	0.0087	0.0091	0.0015
	2	3.14	0.0056	0.25	0.0052	0.0265	0.0028
Between dendrites	3	1.35	0.1186	0.24	0.3068	0.7019	0.031
	4	1.06	0.0336	0.36	0.0064	1.1141	1.0135
	5	1.07	0.2881	1.09	0.0778	3.4538	0.021
	6	0.34	0.054	0.53	0.0134	0.5391	0.082

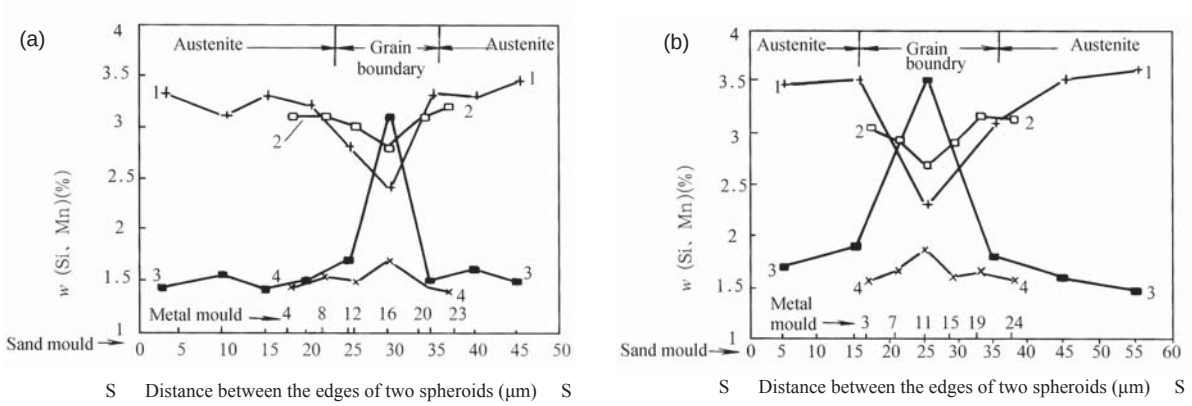

(a) *w*(Mn) = 1.5%, (b) *w*(Mn) = 1.75%, (c) *w*(Mn) = 2.0%;
sample size: *Φ* 32 mm; composition: *w* (C) = 3.3%, *w*(Si) = 2.95%.
1- Si (sand mould), 2 - Si (metal mould), 3 - Mn (sand mould),
4 - Mn (metal mould); S = spheroid.

Fig. 3-90: Effect of Mn content on the segregation tendency of Mn and Si [137]

count, shorten the distance between spheroids and reduce the *LTF* regions. Accordingly, the concentration of C and other positive elements "pushed" to *LTF* regions is decreased. In addition, a high nodule count increases the interface area of austenite shells, thus diluting the concentration of elements distributed at the interfaces. So, with a high nodule count, micro-segregation is obviously reduced, see Fig. 3-91. For two samples with the same composition, but different nodule count, the width of intercellular regions and the concentration of Ni, Si, Mo and C in the intercellular regions are both different. The sample with a lower nodule count (see Fig. 3-91a) has wider intercellular regions with a high Mo concentration; at the same time, the

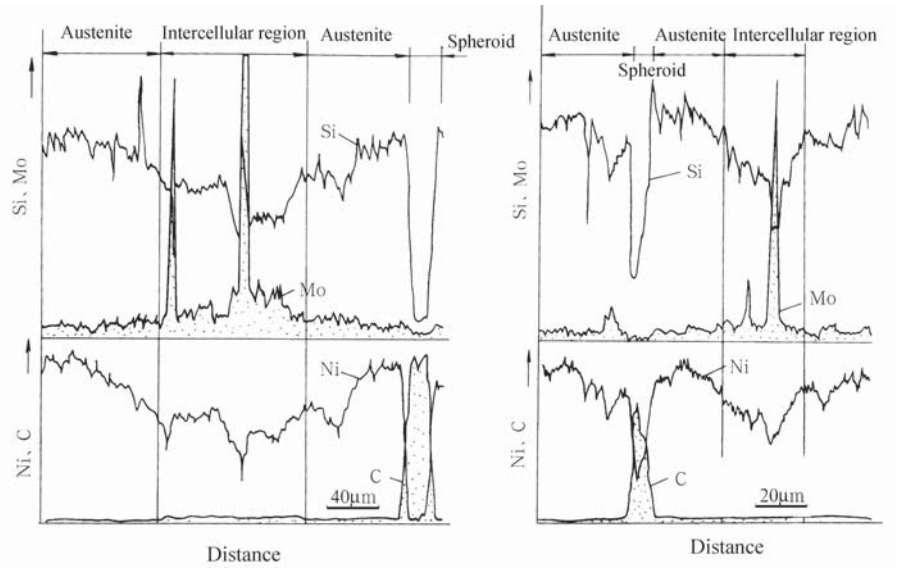

(a) Nodule count – 200 mm^{-2} (b) Nodule count – 1,400 mm^{-2}

Fig. 3-91: Relationship between degree of segregation of Si, Mo, Ni and C to nodule count [128]

concentration of Ni and Si is relatively low.

Thin wall or chilled-mould produced castings have an obvious high nodule count and significantly reduced degree of segregation. For high Mn SG iron, intercellular segregation will significantly decrease mechanical properties, especially the ductility. However, by using a metal mould and increasing the nodule count from 200 mm^{-2} to 1,100 mm^{-2}, the deleterious effect caused by high Mn (w(Mn) = 1.5%), is overcome[137].

(3) Heat treatment

Heat treatment can reduce segregation, but short heating and holding periods do not change the element distribution significantly. This is because the atom radius of elements Si, Ni, Cu, Mo, Cr and Mn is relatively large; these elements are very difficult to diffuse by migration in austenite. If carbides are formed, even homogeneous heat-treating at 980 ºC for 10 hours, will not eliminate them completely [138].

(4) Other factors

Increasing inoculation, increasing carbon equivalent, and adding trace quantities of Bi and Sb can all increase nodule count and thus reduce segregation. For improving the strength and elongation of as-cast SG iron, in-mould inoculation, with the inoculant containing Bi, can be used. With this method, for a 25 mm thick test block, the nodule count can reach 300 mm^{-2}, with a nodule size reducing to 20 μm, thus segregation in the intercellular region is greatly decreased; even with a Mn content reaching 1.16%, 45%–70% of ferrite and elongation > 10% can still be obtained [139]. Also, it is suggested [140] that for castings of section thickness 50 mm, the nodule count should exceed 125–150 mm^{-2} and the diameter of spheroids must be less than 40 μm so as to reduce the negative effects of segregation on ductility and toughness, to the maximum extent.

3.7.3 Effect of segregation on the structure and properties of SG iron

(1) Negative segregation elements

Silicon: Si segregates to austenite and enriches the area around graphite spheroids, enlarges the temperature range of eutectoid transformation and promotes the formation of ferrite. So, most of as- cast structures of unalloyed SG iron consist of graphite spheroids with ferrite shells + pearlite (often called a 'bullseye' structure). This 'bullseye' structure can suppress crack propagation from the surface of graphite spheroids and improve resistance to dynamic load. However, the solid solution strengthening of Si in austenite causes lattice distortion and results in resistance to sliding under ultra-elastic stress; when the uneven distribution of Si is serious, this type of resistance to sliding becomes even more severe. In addition, the enrichment of Si around graphite spheroids promotes the precipitation of secondary graphite during solid phase transformation. Since the region of high Si content has a high eutectoid transformation temperature, this readily causes pearlite in these regions to coarsen during austenite transformation. Therefore, the Si segregation will exert an unfavourable influence on the mechanical properties. Table 3-21 lists the influence of the segregation degree of Si on mechanical properties of two groups of samples with the same nodule count, ferrite content and nodularity [141]. It can be seen that the sample with lower K_s has both improved strength and elongation; both samples have a nodule count of 180–200 mm^{-2} and a volume fraction of 95% ferrite.

Table 3-21: The effect of uneven distribution of Si on mechanical properties [141]

Sample	w (Si%)				Mechanical properties		
	Average of the melt	In the eutectic cells	Between eutectic cells	K_s	UTS, R_m (MPa)	YT, $R_{P0.2}$ (MPa)	Elongation, A (%)
1	2.2	3.2	1.5	2.12	420	290	11.3
2	2.6	3.0	2.1	1.42	460	320	17.9

Copper and Nickel: Ni, Cu and Si are all negative-segregation elements. However, Ni and Cu are different from Si in that they decrease the eutectoid transformation temperature. Also, Cu is enriched at the interface between graphite spheroids and metal matrix [142], thus inhibiting C diffusion. So, Cu and Ni inhibit ferritisation in the region around graphite (which is rich in silicon), thus promoting pearlite. In high Ni SG iron (without Cr), the depletion of Ni and enrichment of Mn at the boundaries of eutectic grains cause a decrease in both ductility and strength [143].

(2) Positive segregation elements

Manganese: Mn is enriched at the boundaries of eutectic cells and when w(Mn)>0.5%, can form Mn_3C. Because the sulphur content in SG iron is low, a small amount of Mn can immediately show the deleterious effect of its positive segregation, thus the allowable content of Mn in SG iron is relatively lower than in grey iron. Although Mn can reduce ferrite in SG iron, since it is depleted around graphite, its effect to suppress a 'bullseye' structure is limited. For example, for a Φ 20 mm test bar with w(C) 3.85% and w(Si)2%, a Mn content as high as 1.3% cannot prevent the formation of ferrite around graphite spheroids. Mn segregates to *LTF* regions and makes the austenite stable in these regions. In ADI, after austempering, a mixed structure of high carbon martensite + retained austenite may form in the *LTF* regions, thus drastically decreasing ductility and strength. Accordingly, the Mn in ADI should be low: w(Mn)<0.2%–0.3%. For high ductility, ferritic SG iron, w(Mn) ≤ 0.2%–0.3% is a proper amount. In pearlitic and ferritic SG irons, the segregation of Mn and Cr leads to an increased tough-brittle transition temperature and is prone to cause brittle fracture; the heavier the section, the more severe the tendency to brittle fracture.

Chromium: Cr has a stronger segregation tendency than Mn and is prone to form intercellular carbide Cr_3C, thus decreasing dynamic load properties and increasing the tendency to form shrinkage porosity [141].

Table 3-22: Relationship between the shape of V_4C_3 and composition [144]

Shape of V_4C_3	Composition (mass %)					Composition feature
	V	Fe	Mo	Mn	Si	
Square	90.90	7.70	0.00	0.61	0.70	without Mo
Cashew	67.83	29.32	0.00	1.21	1.64	without Mo
Triangular	67.92	11.55	17.83	1.91	0.80	with Mo

Vanadium: V has a stronger tendency to form carbide than Cr; w(V)>0.1% can form VC or V_4C_3. Vanadium carbides appear as separated particles, but can also form eutectic or solid solution with iron carbide. When the V content is low, V is present as a limited solid solute in iron carbides. The shape of vanadium carbides is related to their composition, see Table 3-22[144]. Square shaped vanadium carbide (V_4C_3) solid - dissolves Fe, Si and Mn atoms; cashew shaped vanadium carbide (V_4C_3) dissolves relatively more Fe, Si and Mn, whilst triangular vanadium carbide contains large amounts of Mo.

Titanium: Ti is prone to form TiC with C, which contains 20%C and 80%Ti (w%) and has a melting point of 3,180 ℃. TiC appears as isolated blocks and the nearer to the end of solidification, the more the amount of TiC. When the content of Ti exceeds 0.02%, this type of titanium carbide (TiC) can be found in the microstructure of cast iron [33]. When C and N are present in cast iron, Ti easily forms compounds with N and C, but as the titanium compounds are present as isolated blocks, their detrimental effect on mechanical properties is not as significant as the compounds of V, Cr and Mo. However, when forming the acicular, intercellular, multi-carbide of Mo-Ti-V, mechanical properties are reduced in the same way. TiC will also produce harmful effects during machining and this effect should not be ignored.

Molybdenum: Mo is an element which strongly segregates to *LTF* regions. The intercellular structure which is formed is not simple carbide, but a complex one consisting of alloyed carbide containing Mo and Mn, and a compound of Mo-Fe. When phosphorus is slightly higher, Fe-Mo-P compound occurs in the intercellular structure [145]. Mo is also prone to form molybdenum silicates ($MoSi_2$ or Mo_2Si_3) in the intercellular boundaries. As well as significantly decreasing dynamic load properties, these structures also increase micro porosity [127].

In order to overcome the detrimental effect of segregation elements on structure and properties, it is possible to add positive and negative segregation elements together to obtain a desirable uniform structure. Lacaze et al.[146] suggested that a combined addition of w(Mn) = 0.5% and w(Cu) = 1.0% can produce fully pearlitic as-cast SG iron. In the same way, the use of Cu and Mo in ADI can help obtain a uniform austempered structure. This is because Cu preferentially segregates to austenite crystals whilst Mo is enriched outside the austenite, which increases the hardenability of ADI. The strength and ductility obtained from ADI containing Cu and Mo is better than the one containing Mo only.

(3) Phosphorus, sulphur and the elements with low melting point

Phosphorus: P is not a carbide promoting element, but shows a positive segregation tendency. P occurs as iron phosphide, which forms low melting point steadite (ternary phosphide eutectic); it exists in the *LTF* regions and decreases strength and ductility. Phosphorus is slightly soluble in α-Fe and γ-Fe. Phosphorus also segregates to the sub-grain boundaries of austenite and reduces ductility at the interface of sub-grains, compared with the ductility inside the austenite grains, thus increasing annealing brittleness of the SG iron [147]. In order to overcome the detrimental effect of P segregation, Kozlov suggested [148] adding Ce to change the morphology and distribution of phosphide eutectic and thus expand the use of high phosphorus pig iron; this is because the formed cerium phosphide has a high melting point and during the early stage of solidification, forms as isolated round particles, which are dispersed around the eutectic cell boundaries.

Sulphur: S is low in SG iron and occurs mostly as sulphides; the sulphur which exists as solid solution is extremely low. Sulphide inclusions are present in the nuclei of graphite and benefit the formation of graphite nuclei.

Tin and antimony: Low melting point elements Sn and Sb are adsorbed on the interface of graphite and metal; they form a thin film and inhibit the diffusion of carbon atoms to graphite, thus hindering the formation of ferrite [149]. By this mechanism, the ability of Sn and Sb to promote pearlite is stronger than that of Cu or Ni. In grey iron with w(Sn) = 0.03%–0.12% and in SG iron with w(Sn) = 0.01%–0.06%, 100% pearlite can be obtained. Sb has an even stronger pearlite-forming ability than Sn. Excessive Sb and Sn segregate in the *LTF* liquid and form intercellular compounds $FeSn_2$ and $FeSb_2$, giving rise to decreased strength and ductility[33].

References

[1] Fang Keming. Graphite Morphology of Cast Iron and Microstructure Phase Diagrams. Beijing: Science Press, 2000. (in Chinese)

[2] Wallace J F. Effects of Minor Elements on the Structure of Cast Irons. AFS Transactions, 1975, 83: 363–378.

[3] Latich M J, Hitchings J R. Characterization of Inclusions as Nuclei for Spheroidal Graphite in Ductile Cast Iron. AFS Transactions, 1976, 84: 653–664.

[4] Jacobs M H, Law T J, Melford D A and Stowell M J. Identification of heterogeneous nuclei for graphite spheroids in chill-cast iron. Metals Technology, 1976, 3: 98–108.

[5] Zhou Zaoxi. Experimental Studies on Microstructure of Graphite in Cast Iron and Its Inoculation Mechanism [Dissertation]. Mechanical Department, Tsinghua University, Beijing, 1987. (in Chinese)

[6] Askeland D R, Trojan P K and Flinn R A. Investigation of Mechanism of Dross Formation in Ductile Iron. AFS Transactions, 1970, 78: 125–132.

[7] Li Rongde, Yu Haipeng and Ding Hui. Cast Iron Quality and Its

Control Technology. Bejing: China Machine Press, 1998. (in Chinese)
[8] Cochard V, Harding R A, Campbell J and Herold R. Inoculation of Spheroidal Graphite Cast Iron. The Physical Metallurgy of Cast Iron V, (Edited by V G. Lesoult and J.Lacaze), Scite Publ., Switzerland,1997: 277–284.
[9] Biswas P K. Keimbildungstheorie für die Kugelgraphit-Morphologie. Giesserei, 1998(10): 46–59.
[10] Wallace J F.Inoculation-Sulfur Relationship in Cast Iron. AFS Transactions, 1972, 80: 317–320.
[11] Keming F, Ruiming N and Xiaoliang F. Distribution of the Nodularizing Agent Cerium and Subversive Agent Sulphur in Various Phases of Cast Iron. British Foundryman, 1985(3): 127-130.
[12] Yang Jingxiang. The Development of Inoculation Techniques. Modern Cast Iron, 1986(1): 20–24. (in Chinese)
[13] Черновол А В, Абрамова В П,Хуснутдинов Г Д. О Неметалических Включенияхв Чугунах,Модифицированных A1 и S. Иэвестия Академии Наук СССР. Металлы, 1977(3): 26–30.
[14] Heine R W, Loper C R, Jr. Dross Formation in the Processing of Ductile Cast Iron. AFS Transactions, 1966, 74: 274–280.
[15] Askeland D R, Trojan P K, and Flinn R A. Dross Forming Reactions in the System Mg-Si-O in Ductile Iron. AFS Transactions,1972, 80: 349–358.
[16] Weis W. The importance of deoxidation in the crystallization of cast iron. In: The Metallurgy of Cast Iron, B. Lux, I. Minkoff, F. Mollars(eds.), St. Saphorin (Switzerland): Georgi Pub. Co., 1975: 69–80.
[17] Francis B. Heterogeneous Nuclei and Graphite Chemistry in Flake and Nodular Cast Irons. Metall. Trans. A, 1979,10: 21–31.
[18] Tartera J. Cast Iron Inoculation Mechanism. AFS International Cast Metals Journal, 1980 (4): 1–14.
[19] Zeedijk M B. Identification of the Nuclei in Graphite Spheroids by Electron Microscopy. J. Iron Steel Inst.,1965(7): 737–738.
[20] Stefanescu D M. Theory of Solidification and Graphite Growth in Ductile Iron. In: Ductile Iron Handbook, AFS, 1992.
[21] Latona M C, Kwon H W, Wallace J F and Voss J D. Factors Influencing Dross Formation in Ductile Iron Castings. AFS Transactions, 1984, 92: 881–906.
[22] An Yanjun, Wang Chunqi and Yang Jiguang. Investigation on graphite nucleus in grey cast iron inoculated in mould. In: Proceedings of 1986 Beijing International Foundry Conference (Published by Foundry Institution of Chinese Mechanical Engineering Society),1986: 593–610.
[23] Trojan P K, Cuichelaar P J, Bargeron W N and Flinn R A. An Intensive Investigation of Dross in Nodular Cast Iron. AFS Transactions,1968, 76: 323–333.
[24] Lux B. Nucleation of Eutectic Graphite in Inoculated Gray Iron by Saltlike Carbides. Modern Casting, 1964, 54: 41–47.
[25] Schürmnann E. Interpretation von Ergebnissen mikroanalytischer Untersuchungen an magne-siumbehandelten, Langsam und schnell erstarrten Proben aus Gusseisen mit Kugelgraphit. Giesserei-Forschung, 1994(4): 91–95.
[26] Wang chunchi, Fredriksson H. On the Mechanism of Inoculation of Cast Iron. In: Proceedings of 48th International Foundry Congress, Bulgaria, 1981.
[27] Fredriksson H. Inoculation of Iron-base Alloys. Mater. Sci. Eng., 1984, 65: 137–144.
[28] Skaland T, Grong ø and Grong T. A Model for the Graphite Formation in Ductile Cast Iron: Part 1. Inoculation Mechanism. Metallurgical Transactions A, 1993, 24(10): 2321–2345.
[29] Wittmoser A. Zum Gefügeaufbau des Gusseisens mit Kugelgraphit Giesserei Tech. Wiss. Beih., 1952(6–8): 323–334.
[30] Wang Chunqi. Theory and Practice of Cast Iron Inoculation. Tianjin, China: Tianjin University Press, 1991. (in Chinese)
[31] Ball D L. Nucleation of Eutectic Graphite in Cast Iron by Boron Nitride. AFS Transactions, 1967, 75: 428–431.
[32] Yu Haipeng and Yang Jingxiang. Investigation on process of primary crystallization of grey cast iron. Journal of Shenyang Electromechanics College, 1983(2): 37–39. (in Chinese)
[33] Javaid A, Loper C R Jr. Production of Heavy-section Ductile Cast Iron. AFS Transactions, 1995, 103: 135–150.
[34] Kozlov L J, Vorobyev A P. The Role of Rare-earth Metals in the Process of Spheroidal Graphite Formation. Cast Metals, 1991, 4(1): 7–10.
[35] Itofuji H. Keimbildung und Waclistum von Kugel-,Vermicular- bzw Chunkygraphit in magnesiumbehandelten Gusseisenschmelzen. Giesserei, 1996(11): 31–47.
[36] Horie H, Kowata T and Chida A. Influence of Bismuth on Graphite Nodule Count in Thin-Section Spheroidal-Graphite Cast Iron. Cast Metals, 1990, 2(4): 197–202.
[37] Frost J M. Stefanescu D M. Melt Quality Assessment of SG Iron through Computer-aided Cooling Curve Analysis. AFS Transactions, 1992, 100: 189–200.
[38] Horie Hiroshi(ひろし ほりえ). Thin-Walled & High Toughness Ductile Cast Iron. Dalian University of Technology Press, 1992. (in Chinese)
[39] Loper C R Jr, Nandagopal P N and Witter T H. Graphite Pretreatment of Ductile Irons. AFS Transactions, 1988, 96: 671–688.
[40] Liu S L, Loper C R Jr and Witter T H. The Role of Graphite Inoculants in Ductile Iron. AFS Transactions, 1992, 100: 899–906.
[41] Loper C R Jr, Shirvani S and Witter T H. Graphite Inoculants for Gray Cast Iron. In: the Physical Metallurgy of Cast Iron: Proceedings of the Third International Symposium on the Physical Metallurgy of Cast Iron, Stockholm, Sweden, 1984: 89–98.
[42] Qin Ziqiang, Yu Zongsen. Inoculation Mechanism of Cast Iron. Acta Metallurgica Sinica, 1988(1): B 59–61. (in Chinese)
[43] Schubert W D, An Tuan Ta, Kahr G, Benecke T and Lux B. Influence of SiC Additions on the Microstructure of Gray Cast Iron. In: the Physical Metallurgy of Cast Iron: Proceedings of the Third International Symposium on the Physical Metallurgy of Cast Iron, Stockholm, Sweden, 1984: 119–128.
[44] Benecke T, An Tuan Ta, Kalir G, Schubert W D and Lux B. Auflöseverhalten and Vorimpfeffekt von SiC in Gusseisenschmelzen. Giesserei, 1987(10): 301–306.
[45] Stefanescu D M. Cast Iron. In: Metals Handbook, Vol.15, 9th ed., ASM International, Metals Park, OH,1988: 168–181.
[46] Orths K. Deoxidation and Inoculation of Iron-Carbon Casting Alloys and the Deterioration of the Deoxidation Effect with Time. Giesserei, 1980, 20: 620–628.
[47] Itofuji H. Formation Mechanism of Chunky Graphite in Heavy-section Ductile Cast Irons. AFS Transactions, 1990, 98: 429–446.
[48] Horie H,Hiratsuka S, Komata T, et al. Effect of Eight Individual Rare-earth Elements on the Graphite Nodule Count of a Thin-Section of Spheroidal-Graphite Cast Iron. Cast Metals, 1990(2): 73–81.
[49] Jacobs M H, Law T J. Melford D A, et al. Basic processes controlling the nucleation of graphite nodules in chill cast iron. Metals Technology, 1974, 11(11): 490–500.
[50] Onsøien M I, Skaland T and Grong ø. Mechanisms of Graphite Formation in Ductile Cast Iron Containing Cerium and Lanthanum. Int. J. Cast Metals Res., 1999(11): 319–324.
[51] Tartera J, Llorca-lsern N, Marsal M, et al. Confocal Microscope Observation of Graphite Morphology. Int. J. Cast Metals Res, 1999(11): 459–464.
[52] Hummer R. Some aspects of inoculation of flake- and nodular-graphite cast iron. In: The Metallurgy of Cast Iron, B. Lux, I. Minkoff, F. Mollars(eds.), St. Saphorin (Switzerland): Georgi Pub. Co., 1975: 147–160.
[53] Suarez O M, Kendrick R D and Loper C R Jr. A Study of Sulphur Effect in High Silicon Ductile Irons. Int. J. Cast Metals Res., 2000, 13: 135–145.
[54] Skaland T. Ein newer Ansatz zum Impfen von Gußeisen mit

Kugelgraphit. Giesserei-Praxis, 2000 (11): 486–488.
[55] Kusakawa T. Behavior of Oxygen and Nucleation of Graphite in Production of Spheroidal Graphite Cast Iron. In: The Physical Metallurgy of Cast Iron V (Edited by V. G. Lesoult and J. Lacaze). Scite. Publ., Switzerland, 1997: 61–71.
[56] Yang Yunfeng. Metallurgical Physics & Chemistry Conditions of Cast Iron Modification and Inspection Control [Dissertation]. Mechanical Department, Tsinghua University, Beijing, 1985. (in Chinese)
[57] Lux B. Zur Theorie der Bildung von Kugelgraphit in Gußisen. Giesserei-Forschung, 1970(2): 65–80.
[58] Любченко А П. High Strength Cast Iron. (Chinese Version, translated by Zhu Shangjin, Gao Jingyan), Beijing: China Machine Press, 1987.
[59] Horie Hiroshi(ひろし ほりえ). Classification of elements hindering nodularizing of graphite in cast iron. Nodular Cast Iron and Its Inoculation Mechanism, (Chinese Version, Translated and published by Shenyang Research Institute of Foundry), 1978: 204–210.
[60] Hasse S. Die Wirkung von Spurenelementen in Gusseisen mit Kugelgraphit. Giesserei-Praxis, 1995,15 / 16: 271–278.
[61] Wolters D B. Jahresübersicht Guβeisen mit Kugelgraphit (38. Folge). Giesserei, 2001(10): 46–6l.
[62] Morrogh H. The Solidification of Cast Iron and the Interpretation of Results Obtained from Chilled Test Pieces. The British Foundryman, 1960, 53(5): 224–242.
[63] Minkoff I.Crystal Growth Theory and Cast Iron Structures. In: The Physical Metallurgy of Cast Iron Ⅳ(Edited by G. Ohira, T. Kusakawa and E. Niyama), MRS Pittsburg, 1989: 3–13.
[64] Faivre G. On the Mechanisms of Spherulitic Growth in Polymer and Iron Melte. In: The Physical Metallurgy of Cast Iron V (Edited by V. G. Lesoult and J. Lacaze). Scite Publ. Switzerland, 1997: 17–29.
[65] (Russa) Бунин К П, et al. The Structure of Cast Iron. (Chinese Version, translated by Harbin University of Technology), Beijing: China Machine Press, 1977.
[66] Double D D, Hellawell A. Growth structure of various forms of graphite. In: The Metallurgy of Cast Iron, B. Lux, I. Minkoff, F. Mollars (eds.), St. Saphorin (Switzerland): Georgi Pub. Co., 1975: 509–528.
[67] Davis J R. Cast Irons. In: ASM Specialty Handbook, ASM International Materials Park, OH, 1996.
[68] Minkoff I.The Physical Metallurgy of Cast Iron. John Wiley & Sons, Chichester West Sussex, England, 1983.
[69] Александров Н Н. High Quality Cast Iron. (Chinese Version, Translated by Wang Jinhua), Beijing: China Machine Press, 1986.
[70] Chen Xichen. Growth Mechanism of Spheroidal Graphite in Primary Crystallization of Cast Iron. In: Foundry Memoirs, Harbin Institute of Technology (eds.), 1978. (in Chinese)
[71] Вадер З И. Влияние растренного кислорода наформу графита в чугуне. Литейное Производство, 1976(1): 3.
[72] Patterson W, Geilenberg H und Longe B. Anwachsversuche an Graplit-Impfkristallen aus Kohlenstoffgesattigten Eisenschmelzen. Giesserei-Forschung, 1974(3):121–128.
[73] Shenyang Research Institute of Foundry, Dalian Institute of Technology, Shanghai Association for Science and Technology (eds). Nodular Graphite Cast Iron. Beijing: China Machine Press, 1982. (in Chinese)
[74] Minkoff I. The Spherulitic Growth of Graphite. In: Proceedings of the Third International Symposium on the Physical Metallurgy of Cast Iron. Stockholm, Sweden, 1984: 37–45.
[75] Elliott R. Cast Iron Technology. Butterworth's, London, 1988.
[76] Liu Baicheng, et al. SEM study of grphite morphology in cast irons. Nodular Iron, 1980(2): 9–29. (in Chinese)
[77] Yao Yi, Ding Shaolan, Guan Xueming. Transformation of Graphite shape in cast iron and growth kinetics. Acta Metallurgica Sinica, 1986, 22(4): A 358–360. (in Chinese)
[78] Karsay I, Schelleng R D. Heavy Ductile Iron Castings Composition Effect on Graphite Structure. AFS Transactions, 1961, 69: 672–679.
[79] Van de Velde C A. Untersuchungen zum Erstarrungsprozeβ von GGG: in der Deutsche Meelianite-Tagung 1993. Giesserei-Erfahrungsaustausch, 1994(3): 105–108.
[80] Lewensky J A. Conference Examine the Future of Ductile Iron Production. Modern Casting, 1999 (1): 54–56.
[81] Loper C R Jr, Heine R W. Dendritic Structure and Spiking in Ductile Iron. AFS Transactions, 1968, 76: 547–554.
[82] Mulazimoglu M H, Yang Y M, et al. Solidification Studies of Spiking and Large-small Nodule Formation in Ductile Cast Iron Produced by the In-mold Process. AFS Transaction, 1985(93): 627–650.
[83] Zhou Jiyang, Xie Zhuhua, Zhong Fengqi. Austenitic dendrite in ductile iron. Foundry, 1991, 40(3): 9-14. (in Chinese)
[84] Parks T W Jr, Loper C R Jr. A Study of the Conditions Promoting Dendritic Growth in Ductile Iron. AFS Transactions,1969(77): 90–96.
[85] Gagne M, Goller R. Plate Fracture in Ductile Iron Cast. AFS Transactions, 1983(91): 37–46.
[86] Xu Jinjinfeng, et al. Effects of process factors on of the amount and shape of austenitic dendrite in ductile iron. Hot Working Technology, 1998 (1): 30 – 32. (in Chinese)
[87] Zhou jiyang, Schmitz W and Engler S. Untersuchung der Gefugebildung von Gusseisen mit Kugelgraphit bei langsamer Erstarrung. Giesserei-Forschung, 1987, 39(2): 55–70.
[88] Zhou Jiyang. Gefiigebildung von Gusseisen mit Kugelgraphit bei langsamer Erstarrung[Dissertation]. J. Mainz GmbH Verlag, Aachen, Deutschland, 1986.
[89] Cui Qiuya, Xu Jinfeng, Yuan Seng, et al. Austenite Dendrite and Shrinkage Porosity in the Nodular Iron. Foundry, 2001, 50(7): 376–380. (in Chinese)
[90] Zhou Jiyang, Xie Zhuhua, Zhong Fengqi. Effect of austenitic dendrite on mechanical properties in the nodular iron. Acta Metallurgica Sinica, 1992, 28(3): B138–140. (in Chinese)
[91] Lux B. Zur Theorie der Bildung von Kugelgraphit im Guβeisen. Giesserei-Forschung, 1970(4): 161–178.
[92] Lux B, Mollard F and Minkoff I. On the formation of envelopes around graphite in cast iron. In: The Metallurgy of Cast Iron, B. Lux, I. Minkoff, F. Mollars(eds.), St. Saphorin (Switzerland): Georgi Pub. Co., 1975: 371–404.
[93] Li Zhiyuan, et al. Discuss on dislocation and strengthening mechanism in nodular Iron. In: The Proceedings of the Sixth China Foundry Annual Conference, Foundry Institution of Chinese Mechanical Engineering Society, 1985: 280–288. (in Chinese)
[94] Zhou Jiyang, Schmitz W and Engler S. Formation of austenite shell around nodular graphite and its effect on graphite distortion. Acta Metallurgica Sinica, 1989, 25(1): B37–41. (in Chinese)
[95] Zhou jiyang, Schmitz W and Engler S. Formation of Austenite Shell around Nodular Graphite and its Effect on Deterioration of Graphite. AFS Transactions, 1990, 98: 783–786.
[96] Goodrich G M. Cast Iron Microstructure Anomalies and their Causes. AFS Transactions, 1997, 105: 669–683.
[97] Reifferscheid K. Seigerungen in Gusseisen mit Kugelgraphit. Giesserei-Praxis, 1985,17/18: 255–263.
[98] Shiao F T, Lui T S, Chen L H. Eutectic Cell Wall Morphology and Tensile Embrittlement in Ferritic Spheroidal Cast Iron. Metallurgical and Materials Transactions A, 1999, 30(7): 1775–1784.
[99] Engler S. Zur Morphologie erstarrender Eisen-Kohlenstoff-Legierungen. Giesserei techn.-wiss Beihefte, 1966, 17: 169–202.
[100] Stefanescu D M.Funtamentals of solidification of iron-base alloys and composites. In: Proceedings of Technical Forum, CIATF 61st World Foundry Congress, Beijing, 1995: 1–20.
[101] Motz J M, Wolters D B. Über Erstarrungsgefüge and Eigenschaften in dickwandigen Guβeisen mit Kugelgraphit Teil 1: Mikroseigerungen. Giesserei-Forschung, 1988(2): 68–79.
[102] Rivera G L, Boeri R E and Sikora J. A Revealing the Solidification Structure of Nodular Iron. Cast Metals, 1995, 8(1): 1–5.

[103] Mampaey F. Quantification of the Solidification Morphology of Lamellar and Spheroidal Graphite Cast Iron. Int. Journal of Cast Metals Research, 1999(11): 307–312.
[104] Hummer R. Speisungsbedarf und Langenanderungen wahrend der Erstarrung von Gußeisen mit Kugelgraphit-Folgerungen für die Speiserbemessung. Giesserei-Praxis, 1985, 17/18: 241–254.
[105] Hummer R. Beurteillung der Lunkerneigung von Gusseisen mit Kugegraphit mittels Abkühl- und Langenanderungskurven. Giesserei-Praxis,1989(9/10):142–151.
[106] Ellerbrock R, Engler S. Kristallisationsablauf von naheutektischem graphithaltigem Gusseisen. In: der Vortrage eines Symposiums der Deutschen Gesellschaft fur Metallkunde, Erstarrung metallischer Schmelzen,1981: 249–260.
[107] Yeung C E, Zhao H and Lee W B. The Morphology of Solidification of Thin-Section Ductile Iron Castings. Materials Characterization, 1998, 40: 201–208.
[108] Javaid A, Thomson J, Sahoo M and Davis K G. Factors Affecting the Formation of Carbides in Thin-Wall DI Castings. AFS Transactions, 1999, 107: 441–456.
[109] Zhou Zhaoxi, Liu Baicheng, Li Chunli. Interface behavior of some trace elements during crystallization process of graphite in cast iron. In: Proceedings of Cast Iron and its Melting meeting, Foundry Institution of Chinese Mechanical Engineering Society, 1987. (in Chinese)
[110] Banerjee D K, Stefanescu D M. Structural Transitions and Solidification Kinetcs of SG Cast Iron during Directional Solidification Experiments. AFS Transactions, 1991, 99: 747–759.
[111] Zhou Jiyang. Solidification morphology of heavy section ductile iron castings. Foundry, 1996, 45 (1): 1–7. (in Chinese)
[112] Sun G X, Loper C R Jr. Graphite Flotation in Cast Iron. AFS Transactions, 1983, 91: 841–854.
[113] Liu P C, Li C L, Wu D H and Loper C R Jr. SEM Study of Chunky Graphite in Heavy Section Ductile Iron. AFS Transactions, 1983, 91: 119–126.
[114] Zhou Jiyang, Engler S. Chunky Graphite in Heavy Section Ductile Iron. Foundry, 1997, 46(11): 10–17. (in Chinese)
[115] Lux B, Vendl A and Hahn H.Uber die Ausbildung eutektischer Gefuge in grau erstarrten Gußeisen. Radex-Rundschau,1980(1/2): 30–50.
[116] Itofuji H, Masutani A.Nucleation and Growth Behaviour of Chunky Graphite. Int. Journal of Cast Metals Research, 2001, 14: 1–14.
[117] Church N L, Schelleng R D. Detrimental Effect of Calcium on Graphite Structure in Heavy Section Ductue Iron. AFS Transactions, 1970, 78: 5–8.
[118] Tang Chong Xi, Fargues J, Hecht M and Margerie J C. Formation and Prevention of Chunky Graphite in Slowly Cooled Nodular Irons. In: Proceedings of the Third International Symposium on the Physical Metallurgy Cast Iron, Stockholm, Sweden, 1984: 67–76.
[119] Karsay S I, Campomanes E. Control of Graphite Structures in Heavy Section Ductile Iron Castings. AFS Transactions, 1970, 78: 85–92.
[120] Liu B C, Li T X, Rue Z J and Loper C R Jr. The Role of Antimony in Heavy-section Duction Iron. AFS Transactions, 1990, 98: 753–758.
[121] Hayrynen K L, Faubert G P, Moore D J, Rundman K B. Heavy Section ADI: Microsegregation, Microstructure, and Tensile Properties. AFS Transactions, 1989, 97: 747–756.
[122] Burke C M, Moore D J, Rundman K B. Ausforming-Austempered Ductile Iron. AFS Transactions, 1998, 106: 91–97.
[123] Heine R W. Einige Gesichtspunkte zum Erstarrungs-und Speisungsverhalten von Gusseisen mit Kugelgraphit. Giesserei-Praxis, 1995, 13/14: 242–253.
[124] Heine R W. Nodule count: The Benchmark of Ductile Iron Solidification. AFS Transactions, 1993, 101: 879–884.
[125] Liu Shengfa, Zhao Bopan. Study on role of compounded inoculation in non-alloy austenitic-bainitic S.G. lron. Modern Cast Iron, 1998(4): 9–11. (in Chinese)
[126] Hasse S. Duktiles Gusseisen: Handbuch fur Gusserzeuger and Gussverwender. Berlin: Fachverlag Schiele and Schon, 1996.
[127] Marks J R. Metallography of Ductile Iron. AFS Transactions, 1999, 107: 819–827.
[128] Tanaka Y, Kamide H, Hiraoka T, et al. Effect of the Graphite Nodule Count on Mechanical Properties of Austempered Spheroidal Graphite Cast Iron. In: Proceedings of 4th International Symposium on the Physical Metallurgy of Cast Iron, Tokyo, Japan. Sept., 1989: 235–242.
[129] Rivera G, Boeri R and Sikora J. Counting Eutectic Grains in S.G. Cast Iron. The Physical Metallurgy of Cast Iron V (Edited by V. G. Lesoult and J. Lacaze), Scite Publ., Switzerland, 1997.
[130] Rivera G, Boeri R and Sikora J. Influence of the Solidification Microstructure on the Mechanical Properties of Ductile Iron. Int. Journal of Cast Metals Research, 1999, 11: 533–538.
[131] Hass S, Röhig K. Hochfeste Gußeisen mit Kugelgraphit-moderne Werkstoffkonzepte mit Maximalen Eigenschaftskombinationen. Giesserei-Praxis ,1999(4): 154–165.
[132] Selig C, Lacaze J. Study of Microsegregation Build-up during Solidification of Spherodal Graphite Cast Iron. Metallurgical and Materials Transactions B, 2000, 31(8): 827–836.
[133] Karsay I. Gusseisen mit Kugelgraphit. I. Grundlagen-Technologie. QIT-Fer et Titane Inc, 1992.
[134] Boeri R, Weinberg F. Microsegregation in Ductile Iron. AFS Transactions, 1989, 97: 179–184.
[135] Boeri R, Weinberg F. Microsegregation of Alloying Elements in Cast Iron. Cast Metals, 1993(3): 153–158.
[136] Liu P C, Loper C R Jr. Segregation of Certain Elements in Cast Irons. AFS Transactions, 1984, 92: 289–295.
[137] Owhadi A, Hedjazi J, Davami P, et al. Microsegragation of Manganese and Silicon in High Manganese Ductile Iron. Materials Science and Technology, 1997(10): 813–817.
[138] Yeung C F, Zhao H and Lee W B. Effect of Homogenisation Treatment on Segregation of Silicon in Ferritic Ductile Irons: A Colour Metallorgrahic Study. Materials Seience and Technology, 1999, 15(7): 733–737.
[139] Zhou Daoguang, Wu Hongqiang, Lu Wenghua. Effects of Mn Content on Microstructure and Properties of As-cast Ductile Iron. Foundry, 1993, 42(5): 10–14. (in Chinese)
[140] Masse S. Die Notwendigkeit einer Impfbehandlung von perlitischem Gusseisen mit Kugelgraphit im Gusszustand zur Verbesserung der mechanischen Eigenschaften. Giesserei-Praxis, 1995(7/ 8): 124–133.
[141] Motz J. Mikroseigerungen-eine leicht übersehene Einflußgröβe bei der Gefügebeschreibung von Guβwerkstoffen. Praktische Metallographie, 1988, 25: 285–293.
[142] Pan E N, Lou M S and Loper C R Jr. Effects of Copper, Tin and Manganese on the Eutectoid Transformation of Graphitic Cast Irons. AFS Transactions, 1987, 95: 819–840.
[143] Jolley G.Segregation in Nodular Iron and its Influence on Mechanical Properties. The British Foundryman, 1967(3): 79–92.
[144] Zai Qijie. Role of vanadium in cast iron and cast iron containing vanadium. Modern Cast Iron, 2001 (4): 25–28. (in Chinese)
[145] Liu P C, Poper C R Jr. Electron Microprobe Study of Intercellular Compounds in Heavy-Section Ductile Iron. AFS Transactions, 1981, 89: 131–140.
[146] Lacaze J, Boudot A,Gerval V, et al. The Role of Manganese and Copper in the Eutectoid Transformation of Spheroidal Graphite Cast Iron. Metallurgical and Materials Transactions A, 1997, 28(10): 2015–2025.
[147] Лепнер Ю С, Сёреденко В Н. Опричине отпускной Хрупкости в Чугунах сшаровидным графитом. Литейиое Производство, 1988(12): 4–5.
[148] Kozlov L Y, Vorobyer A P, Chen Guiru and Azzam S. Effect of Phosphorus on the Crystallization of the Ductile Iron. In: Proceedings of the 61st World Foundry Congress, Beijing, China, Sept.,1995: 475–486.
[149] Johnson W C, Kovaca B V. The Effect of Additives on the Eutectoid Transformation of Ductile Iron. Metall. Trans. A, 1978(9): 219–229.

To Be continued